A Critical Review for Proper Use of Water/Oil/Gas Transfer Functions in Dual-Porosity Naturally Fractured Reservoirs: Part I

B. Ramirez,* SPE, **H. Kazemi,** SPE, **M. Al-Kobaisi,** SPE, and **E. Ozkan,** SPE, Colorado School of Mines; and **S. Atan,** SPE, Marathon Oil Corporation

Summary

Accurate calculation of multiphase-fluid transfer between the fracture and matrix in naturally fractured reservoirs is a crucial issue. In this paper, we will present the viability of the use of simple transfer functions to account accurately for fluid exchange resulting from capillary, gravity, and diffusion mass transfer for immiscible flow between fracture and matrix in dual-porosity numerical models. The transfer functions are designed for sugar-cube or match-stick idealizations of matrix blocks.

The study relies on numerical experiments involving fine-grid simulation of oil recovery from a typical matrix block by water or gas in an adjacent fracture. The fine-grid results for water/oil and gas/oil systems were compared with results obtained with transfer functions. In both water and gas injection, the simulations emphasize the interaction of capillary and gravity forces to produce oil, depending on the wettability of the matrix.

In gas injection, the thermodynamic phase equilibrium, aided by gravity/capillary interaction and, to a lesser extent, by molecular diffusion, is a major contributor to interphase mass transfer. For miscible flow, the fracture/matrix mass transfer is less complicated because there are no capillary forces associated with solvent and oil; nevertheless, gravity contrast between solvent in the fracture and oil in the matrix creates convective mass transfer and drainage of oil.

Using the transfer functions presented in this paper, fracture- and matrix-flow calculations can be decoupled and solved sequentially—reducing the complexity of the computation. Furthermore, the transfer-function equations can be used independently to calculate oil recovery from a matrix block.

Introduction

Naturally fractured reservoirs contain a great amount of the known petroleum hydrocarbons worldwide and, hence, are an important source of energy fuels. However, the oil recovery from these reservoirs has been rather low. This low level of oil recovery points to the need for accurate reservoir characterization, realistic geological modeling, and accurate flow simulation of naturally fractured reservoirs to determine the locations of bypassed oil.

Reservoir simulation is the most practical method of studying flow problems in porous media when dealing with heterogeneity and the simultaneous flow of different fluids. In modeling fractured systems, a dual-porosity concept is typically used to idealize the reservoir on the global scale. In the dual-porosity concept, the bulk of the fluid transport takes place at high velocities in the fractures from one grid cell to another irrespective of flowing phase. On the other hand, in two- or three-phase flow, there is usually a local exchange of fluids between the fractures and the adjacent matrix at comparatively low velocities. The issue of fluid velocities is very critical in naturally fractured reservoirs because, in multiphase flow, typically water or gas can move rapidly in the fractures and surround the matrix blocks partially or totally. Once a matrix block is surrounded partially or totally by a particular fluid, transfer of fluid phases and components takes place between the fracture and matrix, which is the focus of this paper. In particular, deciphering the exchange mechanisms and describing the pertinent equations of mass transfer constitute the heart of this paper. Similar issues are relevant to any variant of the dual-porosity concept, such as the triple-porosity, irrespective of the idealization concept.

Physical Perspective

First, let us consider a naturally fractured reservoir containing a single-phase fluid, such as gas. For this case, the reservoir is produced by fluid expansion by means of production wells. The production mechanism is rather simple in that the producing well creates a pressure gradient in the fractures connected to the well that, in turn, create a pressure drawdown on the adjacent matrix to create matrix flow. In this scenario, all connected fractures play a role in bringing gas to the wells. In fact, the early models of Barenblatt et al. (1960) and Warren and Root (1963) pertain to this mechanism. We should note that, in these publications, the driving force for matrix depletion is the pressure differential between the fracture and matrix only.

Second, let us consider water/oil flow in a fractured reservoir. In this case, water from an injection well or from the aquifer can easily flow through the fracture network much faster than through the matrix. This can be demonstrated by simply imposing a horizontal constant pressure gradient across a thin partially or completely oil-wet matrix block containing a high conductivity fracture and then calculating the interstitial velocity of the water phase in the fracture and matrix. If the matrix block is thick, then gravity difference between water and oil can lead to oil production by gravity drainage, if the gravity can overcome the capillary pressure of the rock. This scenario often applies to a large percentage of the oil-wet carbonate reservoirs in the world. Finally, if the matrix is water-wet, the water imbibes into the matrix to release oil. Thus, the rock wettability and block size play major roles in fluid exchange between the fracture and matrix. Similar arguments can be made for the situation in which a high-mobility gas surrounds a matrix block. Knowing that gas is the nonwetting phase, one could resort to the gravity force to overcome the capillarity resistance to the invading gas.

Third, many large petroleum reservoirs in the world are associated with an active aquifer and, then, after the initial production by depletion drive, these reservoirs create a secondary gas cap. At this stage of the reservoir life, more than half of the mobile oil is still locked in the matrix blocks and the aquifer water and the gas-cap gas curtail the oil productivity of the wells. Obviously, we would like to find ways to produce part of the remaining oil and improve the oil-production rate from the wells. Unfortunately, not many practical options are available to achieve this goal. One option is to inject a surfactant in the water phase to change the

*Now with Marathon Oil Corporation.

This paper (SPE 109821) was accepted for presentation at the SPE Annual Technical Conference and Exhibition, Anaheim, California, USA, 11–14 November 2007, and revised for publication. Original manuscript received for review 2 August 2007. Revised manuscript received for review 28 May 2008. Paper peer approved 22 July 2008.

wettability and lower the oil/water interfacial tension. The second option is to inject gas strategically (e.g., to increase reservoir pressure, oppress water encroachment, reduce gas/oil interfacial tension, or invoke gas/oil gravity drainage in the right places). Thus, in multiphase flow it is not the pressure gradient that dominates flow—it is a combination of several local forces and their interaction that controls oil production.

Fourth, we are always concerned with accuracy and the speed of computation. For accuracy, employing a fine-grid simulation should create a more accurate account of flow between the matrix and fracture. However, this cannot be performed for all matrix blocks because it will lead to billions of cells in a reservoir model. The transfer-function approach provides a practical solution because the data requirement is substantially lower and the speed of computation is much faster. However, to have a credible replacement for fine gridding of individual matrix blocks, the transfer-function approach must produce results nearly as accurate as the fine-grid simulation.

Fifth, the transfer functions are zero-dimensional mathematical expressions that are designed to account for the transfer of fluids and components between a 3D matrix block and its surrounding fractures. The zero-dimensionality works well for single-phase flow, but it does not work well for immiscible flow and miscible flow with contrasting densities between the fractures and matrix. In gravity/capillary-dominated flow, we can provide the transfer functions with a pseudodimensionality in the vertical direction. This approach is closely related to the classical 1D gravity-drainage formulation (Hagoort 1980, Al-Kandari et al. 2002). As shown in the latter work, the pure oil/gas-gravity-drainage equation is

$$-\hat{u}\frac{\partial \hat{f}_o}{\partial z}+\frac{\partial}{\partial z}\left(\hat{D}_{pc}\frac{\partial S_o}{\partial z}\right)=\frac{\partial S_o}{\partial t}, \quad (1)$$

where,

$$\hat{f}_o=\frac{k_{rog}}{k^*_{rog}}, \quad (2)$$

$$\hat{u}=\frac{k}{\phi}\frac{k^*_{rog}}{\mu_o}\left(\gamma_o-\gamma_g\right)\frac{\partial D}{\partial z}, \quad (3)$$

and

$$\hat{D}_{pc}=\frac{k}{\phi}\lambda_o\frac{\partial p_{cog}}{\partial S_g}. \quad (4)$$

Substituting Eqs. 2, 3, and 4 into Eq. 1, the following equation is obtained, which is an analog of the gas/oil transfer function:

$$-\frac{\partial}{\partial z}\left\{k_m\lambda_o\left[\left(\gamma_o-\gamma_g\right)+\frac{\partial p_{cgom}}{\partial z}\right]\right\}=\phi_m\frac{\partial S_o}{\partial t}. \quad (5)$$

Finally, in single-phase flow, the computing grid dimensions could be smaller than the matrix block, while in multiphase flow the vertical dimension of the grid should not be smaller than the matrix-block height. In the latter, it is best to use a fine-grid simulation of the matrix blocks in the vertical coordinate to match that of the fractures. This approach is a special version of the "dual-porosity/dual-permeability formulation," but because the fine gridding of the matrix block is performed in the vertical coordinate only, the computation work can be reduced efficiently to a conventional 3D, three-phase equivalent.

Literature Review

The heart of dual-porosity multiphase-flow modeling is the transfer function that accounts for the transfer of fluids between the fracture and the matrix (Barenblatt et al. 1960; Warren and Root 1963; Kazemi et al. 1976; Litvak 1985; Sonier et al. 1988; Gilman and Kazemi 1988; Balogun et al. 2007).

The foundations of the current models were laid by Barenblatt et al. (1960) and Warren and Root (1963). These authors dealt with the mathematical formulation of single-phase flow in dual-porosity systems. The material-balance equation described by the transfer function, τ, defined as the flow rate per unit volume of rock, had this general form:

$$\tau=\sigma\frac{k}{\mu}\left(p_f-p_m\right), \quad (6)$$

where σ is the shape factor; k is matrix permeability; μ is fluid viscosity; and $(p_f - p_m)$ is the pressure difference between the fracture and the matrix. Warren and Root (1963) provided an analytical solution for radial flow for well-testing purposes and idealized a fractured reservoir as a set of stacked sugar cubes. Kazemi et al. (1976) extended the Warren and Root (1963) model to water/oil flow and developed a numerical algorithm to solve the fracture-flow equations while accounting for matrix/fracture fluid transfer by use of a multiphase transfer function.

Hydrocarbon reservoirs produce fluids under a combination of mechanisms that include capillarity, gravity drainage, viscous displacement, pore compaction, and fluid expansion. Depending on the flowing phases present, capillary and gravity forces are generally dominant in fractured reservoirs. These forces can work in tandem or can oppose each other (Gilman 2003).

Sonier et al. (1988) and Litvak (1985) provided a dynamic approach to improve the modeling of the interaction of gravity and capillary forces in the matrix/fracture system without fine gridding. Gilman (1986), however, used a fine-grid approach to develop a more accurate method to account for gravity forces better.

Another issue is the viscous displacement in the matrix blocks of the dual-porosity models. Gilman and Kazemi (1988) presented a formulation to account for this effect. Viscous displacement is much more significant in single-porosity systems.

Results from imbibition experiments (Mattax and Kyte 1962), centrifuge experiments (Kyte 1970), physical models (Kleppe and Morse 1974), fractured-core floods (Kazemi and Merrill 1979), stacked cores (Horie et al. 1990), and newer imbibition experiments (Morrow et al. 1995) provided the foundation for scaling laboratory results to field conditions.

Fung (1991) and Uleberg and Kleppe (1996) dealt with the finer details of simulating gravity drainage in dual-porosity reservoirs including the effect of oil reinfiltration from one block to a block underneath, which could lead to lower oil recovery from the fractures in specific conditions.

The magnitude of capillary pressure in the fracture is difficult to assess. However, if one assumes that there is some capillary continuity between matrix blocks across the fractures, then a match-stick dual-permeability model can be used as opposed to the dual-porosity model (Fung 1991).

Additional light was shed on the mechanism of oil production from naturally fractured reservoirs by Saidi (1983), Kazemi et al. (1993), Lekberg and Kleppe (1996), Al-Kandari (2002), and Lu et al. (2006).

Research results are also available from laboratory investigations and related numerical simulations of fractured systems on a single matrix block (Blair 1964; Iffly et al. 1972; Klepe and Morse 1974). Yamamoto et al. (1971) developed the earliest compositional model for studying recovery mechanisms from single matrix blocks surrounded by different fluids.

Shape Factor

There has been much discussion in the literature on the functional form of the shape factor. Shape factor is a geometric factor characteristic of the geometry and boundary conditions of the matrix block. In fact, we propose that the shape factor is generally phase-sensitive. For instance, for the same reservoir, in single-phase flow, the effective matrix-block dimensions are generally smaller, while for multiphase flow, the effective matrix-block dimensions are larger because a displacing fluid, such as gas, tends to finger through larger fractures to surround more of the matrix rock. Similar arguments can be applied to the effective block height because of film flow between blocks in the vertical direction and vertical reinfiltration of oil from one block to another.

An expression for shape factor was presented by Warren and Root (1963) as follows:

$$\sigma = \frac{4n(n+2)}{l^2}, \quad \ldots\ldots (7)$$

where n is the number of normal sets of fractures and l is the characteristic length of a matrix block,

$$l = \begin{cases} L_x, & n=1 \\ 2L_xL_y/\left(L_x+L_y\right), & n=2 \\ 3L_xL_yL_z/\left(L_xL_y+L_yL_z+L_zL_x\right), & n=3 \end{cases} \quad \ldots\ldots (8)$$

Kazemi et al. (1976) later proposed a shape-factor expression based on standard seven-point finite difference:

$$\sigma = 4\left[\frac{1}{L_x^2}+\frac{1}{L_y^2}+\frac{1}{L_z^2}\right], \quad \ldots\ldots (9)$$

where L_x, L_y, and L_z represent the dimensions of a matrix block. The coefficient 4 in Eq. 9 can be replaced by π^2 using the analytical solution of pressure diffusion in a parallepiped-shaped matrix block (Kazemi and Gilman 1993; Chang 1993; Lim and Aziz 1995).

Kazemi et al. (1992) and Morrow et al. (1995), respectively, used the following shape-factor equation for reservoir modeling and for correlating water-imbibition oil recovery from laboratory experiments.

$$\sigma = \frac{1}{V}\sum_{j=1}^{J}\frac{A_j}{d_j}, \quad \ldots\ldots (10)$$

where A_j represents the area for the open surface j of the matrix block; d_j represents the distance from the center of the matrix block to the open surface j; J is the total number of open surfaces; and V is the volume of the matrix block. Eq. 10 reduces to Eq. 9 for sugar-cube or match-stick models and its validity was confirmed recently by Heinemann and Mittermeir (2006). Rangel-German and Kovscek (2003) consider shape factor to be a matching parameter that changes with flow regimes and, hence, a function of time.

Transfer Function and Gravity Shape Factor

The general approach to modeling matrix/fracture fluid transfer is by means of a simple transfer function for a single matrix block surrounded by fractures. This transfer function should account for imbibition, gravity drainage, fluid expansion, and molecular diffusion. Then, the transfer function becomes a major building block for dual-porosity/dual-permeability simulation of naturally fractured reservoirs.

It can be shown that for water/oil flow, the transfer function based on the conventional single-porosity formulation (Kazemi et al. 1976) has the following form for the water phase:

$$\tau_w = \sigma\frac{k_m k_{rw}}{\mu_w}\left\{\left[p_f-p_m\right]-\left(\frac{\sigma_z}{\sigma}\right)\gamma_w\left(D_f-D_m\right)\right\}, \quad \ldots\ldots (11)$$

and

$$\tau_w = \phi_m\frac{\partial S_{wm}}{\partial t}+\phi_m S_{wm}\left(c_{wm}+c_{\phi m}\right)\frac{\partial p_{wm}}{\partial t}. \quad \ldots\ldots (12)$$

The gravity term in Eq. 11 resulted from a mathematical extension of single-phase-flow theory and requires an objective analysis by adhering to the local physics of multiphase interactions. For instance, for water/oil flow, the gravity term in Eq. 11 should be a function of both the height of the matrix block and the contrast between the fluid dynamic forces between the fracture and matrix. This was first recognized by Litvak (1985), later by Sonier et al. (1988), and eventually by Kazemi and Gilman (1993). As a follow-up to these early developments, in Balogun et al. (2007) it is shown that Eq. 11 becomes

$$\tau_w = \sigma\frac{k_m k_{rw}}{\mu_w}\left\{\left[p_f-p_m\right]+\left(\frac{\sigma_z}{\sigma}\right)\gamma_w\left(h_{wf}-h_{wm}\right)\right\}. \quad \ldots\ldots (13)$$

In a later section, we will present other forms of Eq. 13 that will include rock and fluid expansion and molecular diffusion. Gas diffusion in and out of the matrix block involves interphase-mass-transfer and phase-equilibrium calculations (Hoteit and Firoozabadi 2006), which will be presented in a later section.

Finite-Difference Model

Fluid flow in reservoirs is typically modeled numerically by finite-difference discretization of the continuity equation and Darcy's law. For reference purposes, we first focus on water/oil flow to demonstrate the fluid mechanics of the fracture/matrix mass transfer. Then, we will include water/oil/gas flow and compositional effects.

Fig. 1 depicts a schematic of a segment of a naturally fractured reservoir (Beliveau 1989). For numerical modeling, the fracture/matrix reservoir segment in Fig. 1 can be idealized by a model similar to the sketch shown in **Fig. 2** (Civan and Rasmussen 2002).

Fig. 2 is a representation of a grid cell in a dual-porosity reservoir model that consists of a network of fractures surrounding matrix blocks of various sizes. In this paper, we study oil-recovery predictions from only one of the matrix blocks. **Fig. 3** presents the gas/oil capillary/gravity-force balance for a single-cell matrix block for which fluid exchange is approximated with a simple transfer function, τ_g. A detailed fine-grid model of the same matrix block using the relevant flow equations is presented in a later section.

Single-Porosity Water/Oil/Gas Formulation

In this section, the flow equations to model water/oil/gas flow are presented. These equations are used to model the fracture/matrix interaction in a fine-grid, single-porosity setting.

Pressure and Velocity Equations. The total pressure equation for water/oil/gas flow is given by

$$\left\{\begin{array}{l}\nabla\cdot k\left[\begin{array}{l}\lambda_T\nabla p_o-\left(\lambda_w\gamma_w+\lambda_o\gamma_o+\lambda_g\gamma_g\right)\nabla D\\ -\lambda_w\nabla p_{cwo}+\lambda_g\nabla p_{cgo}\end{array}\right]\\ +\hat{q}_T\end{array}\right\} = \phi c_T\frac{\partial p_o}{\partial t}, \quad \ldots\ldots (14)$$

where

$$\lambda_T = \lambda_w+\lambda_o+\lambda_g, \quad \ldots\ldots (15)$$

$$\hat{q}_T = \hat{q}_w+\hat{q}_o+\hat{q}_g, \quad \ldots\ldots (16)$$

and

$$c_T = c_\phi+S_wc_w+S_oc_o+S_gc_g. \quad \ldots\ldots (17)$$

After solving the pressure equation, the following equation can be used to calculate the total velocity of the flowing phases:

$$\vec{v}_T = \vec{v}_o+\vec{v}_w+\vec{v}_g, \quad \ldots\ldots (18)$$

or

$$\vec{v}_T = -\left\{\begin{array}{l}\nabla\cdot k\left[\lambda_T\nabla p_o-\left(\lambda_w\gamma_w+\lambda_o\gamma_o+\lambda_g\gamma_g\right)\nabla D\right]\\ -\nabla\cdot k\lambda_w\nabla p_{cwo}+\nabla\cdot k\lambda_g\nabla p_{cgo}\end{array}\right\}. \quad \ldots\ldots (19)$$

Saturation Equations. Water, oil, and gas saturations are defined by the flow equations for each phase:

$$-\nabla\cdot\vec{v}_w+\hat{q}_w = \phi\frac{\partial S_w}{\partial t}+\phi S_w\left(c_w+c_\phi\right)\frac{\partial p_w}{\partial t}, \quad \ldots\ldots (20)$$

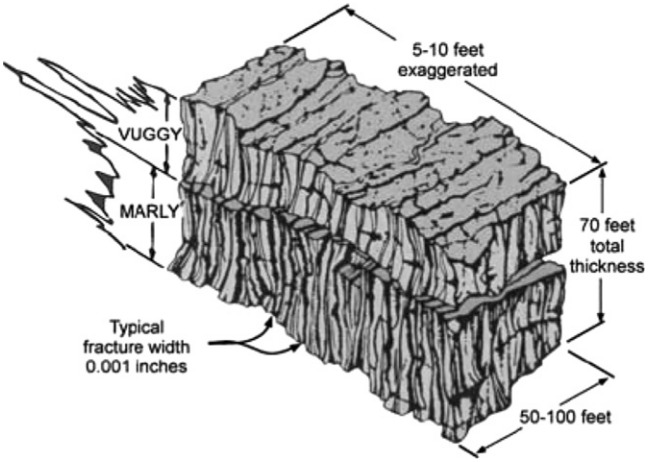

Fig. 1—Schematic of a segment of a naturally fractured reservoir, after Beliveau (1989).

$$-\nabla\cdot\vec{v}_o+\hat{q}_o=\phi\frac{\partial S_o}{\partial t}+\phi S_o\left(c_o+c_\phi\right)\frac{\partial p_o}{\partial t}, \quad \ldots\ldots\ldots (21)$$

and

$$-\nabla\cdot\vec{v}_g+\hat{q}_g=\phi\frac{\partial S_g}{\partial t}+\phi S_g\left(c_g+c_\phi\right)\frac{\partial p_g}{\partial t}. \quad \ldots\ldots\ldots (22)$$

Flux Across Fracture/Matrix Interface. Fluid rates in and out of the matrix block (for the fine-grid model) are calculated at all open boundaries using the product of the phase Darcy velocities at the boundaries and respective cross-sectional areas. For example, the water, oil, and gas rates can be calculated, respectively, as follows:

$$q_w=v_wA, \quad \ldots\ldots\ldots (23)$$

$$q_o=v_oA, \quad \ldots\ldots\ldots (24)$$

and

$$q_g=v_gA, \quad \ldots\ldots\ldots (25)$$

or

$$q_w=-T_w(\nabla p_w-\gamma_w\nabla D), \quad \ldots\ldots\ldots (26)$$

$$q_o=-T_o(\nabla p_o-\gamma_o\nabla D), \quad \ldots\ldots\ldots (27)$$

and

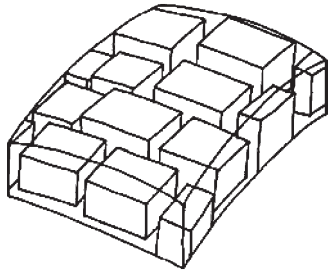

Fig. 2—Idealization of a naturally fractured reservoir, after Civan et al. (2002).

$$q_g=-T_g\left(\nabla p_g-\gamma_g\nabla D\right). \quad \ldots\ldots\ldots (28)$$

Oil recovery is then calculated by a simple time integration of the oil-production rate.

Dual-Porosity Water-/Oil-/Gas-Flow Formulation

The dual-porosity formulation has many benefits, including a more realistic description of high velocity fracture flow and substantial reduction of the number of computing gridpoints.

Pressure Equation. The pressure equation used in modeling water/oil/gas flow in naturally fractured reservoirs is

$$\left\{\begin{array}{l}\nabla\cdot k_f\left[\begin{array}{l}\lambda_{Tf}\nabla p_{o_f}-\left(\lambda_{wf}\gamma_w+\lambda_{of}\gamma_o+\lambda_{gf}\gamma_g\right)\nabla D_f\\ -\lambda_{wf}\nabla p_{cwof}+\lambda_{gf}\nabla p_{cgof}\end{array}\right]\\ -\left(\tau_w+\tau_o+\tau_g\right)+\hat{q}_{Tf}\end{array}\right\}$$
$$=\left(\phi c_T\right)_f\frac{\partial p_{of}}{\partial t}. \quad \ldots\ldots\ldots (29)$$

Saturation Equations. The saturation equations for dual-porosity flow are

$$-\nabla\cdot\vec{v}_{wf}-\tau_w+\hat{q}_{w_f}=\phi_f\frac{\partial S_{wf}}{\partial t}+\phi_f S_{wf}\left(c_{wf}+c_{\phi f}\right)\frac{\partial p_{wf}}{\partial t}, \quad \ldots\ldots\ldots (30)$$

$$-\nabla\cdot\vec{v}_{of}-\tau_o+\hat{q}_{o_f}=\phi_f\frac{\partial S_{of}}{\partial t}+\phi_f S_{of}\left(c_{of}+c_{\phi f}\right)\frac{\partial p_{of}}{\partial t}, \quad \ldots\ldots\ldots (31)$$

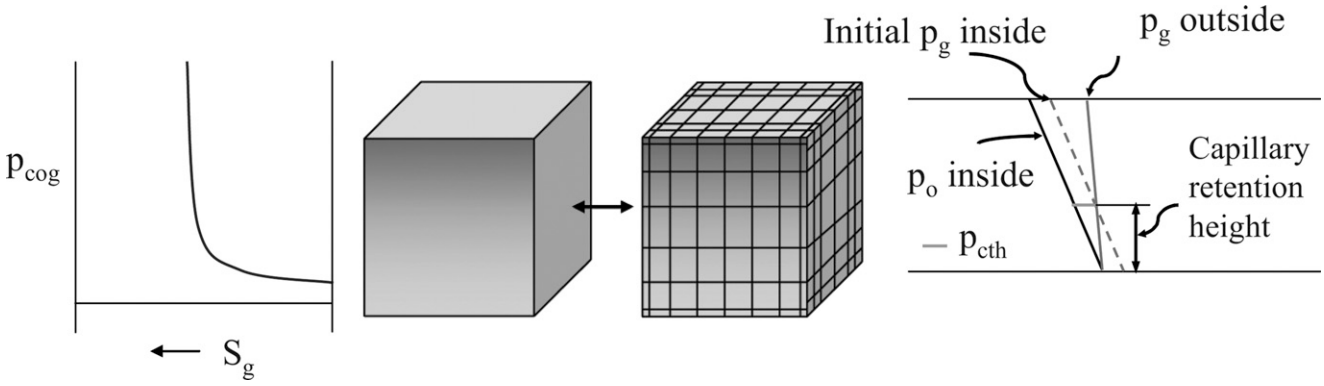

Fig. 3—Schematic of gas/oil capillary-/gravity-force balance for a matrix block.

$$-\nabla\cdot\vec{v}_{gf}-\tau_g+\hat{q}_{g_f}=\phi_f\frac{\partial S_{gf}}{\partial t}+\phi_f S_{gf}\left(c_{gf}+c_{\phi f}\right)\frac{\partial p_{gf}}{\partial t},\quad\ldots\ldots(32)$$

where

$$\tau_w=\tau_{wo}=\left\{\begin{array}{l}\sigma k_m\left(\frac{\lambda_{wf/m}\lambda_{om/f}}{\lambda_T}\right)\left[\begin{array}{l}\left(p_{cwom}-p_{cwof}\right)\\+\left(\frac{\sigma_z}{\sigma}\right)\left(\gamma_w-\gamma_o\right)\left(h_{wf}-h_{wm}\right)\end{array}\right]\\+\left(\frac{\lambda_{wf/m}}{\lambda_T}\right)\left[\begin{array}{l}\phi_m c_{Tm}\frac{\partial p_{om}}{\partial t}\\-\phi_m S_{wm}\left(c_{wm}+c_{\phi m}\right)\frac{\partial p_{cwom}}{\partial t}\end{array}\right]\end{array}\right\},\quad\ldots\ldots(33)$$

$$\tau_g=\tau_{go}=\left\{\begin{array}{l}\sigma k_m\left(\frac{\lambda_{gf/m}\lambda_{om/f}}{\lambda_T}\right)\left[\begin{array}{l}-\left(p_{cgom}-p_{cgof}\right)\\+\left(\frac{\sigma_z}{\sigma}\right)\left(\gamma_o-\gamma_g\right)\left(h_{gf}-h_{gm}\right)\end{array}\right]\\+\left(\frac{\lambda_{gf/m}}{\lambda_T}\right)\left[\begin{array}{l}\phi_m c_{Tm}\frac{\partial p_{om}}{\partial t}\\-\phi_m S_{gm}\left(c_{gm}+c_{\phi m}\right)\frac{\partial p_{cgom}}{\partial t}\end{array}\right]\end{array}\right\},\quad\ldots\ldots(34)$$

$$\tau_o=-\left(\tau_{go}+\tau_{wo}\right)+\phi_m c_{Tm}\frac{\partial p_{om}}{\partial t},\quad\ldots\ldots(35)$$

and

$$\tau_o=\phi_m\frac{\partial S_{om}}{\partial t}+\left(S_{om}\phi_m\right)\left(c_{\phi m}+c_{om}\right)\frac{\partial p_{om}}{\partial t}.\quad\ldots\ldots(36)$$

Additionally,

$$\hat{q}_{Tf}=\hat{q}_{wf}+\hat{q}_{of}+\hat{q}_{gf},\quad\ldots\ldots(37)$$

$$\lambda_T=\lambda_{wf/m}+\lambda_{om/f}+\lambda_{gf/m},\quad\ldots\ldots(38)$$

$$h_{wf}=\left(\frac{S_{wf}-S_{wrf}}{1-S_{wrf}-S_{orf}}\right)L_z=S_{wD}L_z,\quad\ldots\ldots(39)$$

$$h_{of}=\left(\frac{S_{of}-S_{orf}}{1-S_{wrf}-S_{orf}}\right)L_z=S_{oD}L_z,\quad\ldots\ldots(40)$$

and

$$h_{gf}=\left(\frac{S_{gf}}{1-S_{wrf}-S_{orf}}\right)L_z=S_{gD}L_z.\quad\ldots\ldots(41)$$

The implementation of Eqs. 29 through 32 is very easy in the implicit-pressure/explicit-saturation (IMPES) formulation because it eliminates the phase pressures. Furthermore, this form clearly shows the interaction between gravity and capillarity. Finally, this form allows the use of the IMPES, instead of a fully implicit formulation for a dual-porosity reservoir.

Single-Porosity Compositional Formulation

The flow equations for three-phase compositional formulation are presented because they are relevant to the fine-grid simulation and the issue of molecular-diffusion vs. convective-dispersion mixing of components:

$$\left\{\begin{array}{l}\nabla\cdot\left[x_c\xi_o\lambda_o k_f\left(\nabla p_o-\gamma_o\nabla D\right)\right]-\nabla\cdot\left(J^{\mathrm{Mol}}_{o,c}+J^{\mathrm{Disp}}_{o,c}\right)\\+\nabla\cdot\left[y_c\xi_g\lambda_g k_f\left(\nabla p_g-\gamma_g\nabla D\right)\right]-\nabla\cdot\left(J^{\mathrm{Mol}}_{g,c}+J^{\mathrm{Disp}}_{g,c}\right)\\+\nabla\cdot\left[w_c\xi_w\lambda_w k_f\left(\nabla p_w-\gamma_w\nabla D\right)\right]-\nabla\cdot\left(J^{\mathrm{Mol}}_{w,c}+J^{\mathrm{Disp}}_{w,c}\right)\end{array}\right\}$$
$$+\hat{q}_{T,c}=\frac{\partial}{\partial t}\left(\phi z_c/v_T\right),\quad\ldots\ldots(42)$$

for $c=1, 2\ldots N_c+1$.

To solve the above equations, the initial and boundary conditions are needed as are a set of pertinent thermodynamic constraints. These additional requirements are discussed in many publications—notably by Acs et al. (1985); Watts (1986); and Wong et al. (1990); thus, we refer the reader to these publications.

Dual-Porosity Compositional Formulation

The following equations are derived by extending the conventional volume-balance compositional formulation (Acs et al. 1985; Watts 1986; Wong et al. 1990) to dual-porosity systems:

Fracture Flow.

$$\left\{\begin{array}{l}\nabla\cdot\left[x_{cf}\xi_{of}\lambda_{of}k_f\left(\nabla p_{of}-\gamma_{of}\nabla D\right)\right]-\nabla\cdot\left(J^{\mathrm{Mol}}_{o,c,f}+J^{\mathrm{Disp}}_{o,c,f}\right)\\+\nabla\cdot\left[y_{cf}\xi_{gf}\lambda_{gf}k_f\left(\nabla p_{gf}-\gamma_{gf}\nabla D\right)\right]-\nabla\cdot\left(J^{\mathrm{Mol}}_{g,c,f}+J^{\mathrm{Disp}}_{g,c,f}\right)\\+\nabla\cdot\left[w_{cf}\xi_{wf}\lambda_{wf}k_f\left(\nabla p_{wf}-\gamma_{wf}\nabla D\right)\right]-\nabla\cdot\left(J^{\mathrm{Mol}}_{w,c,f}+J^{\mathrm{Disp}}_{w,c,f}\right)\end{array}\right\}$$
$$-\tau_{T,c,f/m}+\hat{q}_{T,c,f}=\frac{\partial}{\partial t}\left(\frac{\phi z_{cf}}{v_{T,f}}\right),\quad\ldots\ldots(43)$$

for $c=1, 2\ldots N_c+1$.

Matrix Flow.

$$\tau_{T,c,f/m}=\frac{\partial}{\partial t}\frac{\phi z_{cm}}{v_{T,m}},\quad\ldots\ldots(44)$$

for $c=1, 2\ldots N_c+1$.

Pressure Equations. ***Fracture Pressure Equation.***

$$\sum_{c=1}^{N_c+1}\bar{v}_{T,c,f}U_{c,f}+\sum_{c=1}^{N_c+1}\bar{v}_{T,c,f}\tau_{T,c,f/m}=\phi_f\left(c_\phi+c_{vT}\right)_f\frac{\partial p_f}{\partial t}.\quad\ldots\ldots(45)$$

Matrix Pressure Equation.

$$\sum_{c=1}^{N_c+1}\bar{v}_{T,c,m}\tau_{T,c,f/m}=\phi_m\left(c_\phi+c_{vT}\right)_m\frac{\partial p_m}{\partial t}.\quad\ldots\ldots(46)$$

In Eqs. 45 and 46,

$$U_{c,f}=\left\{\begin{array}{l}\nabla\cdot\left[x_{cf}\xi_{of}\lambda_{of}k_f\left(\nabla p_{of}-\gamma_{of}\nabla D\right)\right]-\nabla\cdot\left(J^{\mathrm{Mol}}_{o,c,f}+J^{\mathrm{Disp}}_{o,c,f}\right)\\+\nabla\cdot\left[y_{cf}\xi_{gf}\lambda_{gf}k\left(\nabla p_{gf}-\gamma_{gf}\nabla D\right)\right]-\nabla\cdot\left(J^{\mathrm{Mol}}_{g,c,f}+J^{\mathrm{Disp}}_{g,c,f}\right)\\+\nabla\cdot\left[w_{cf}\xi_{wf}\lambda_{wf}k\left(\nabla p_{wf}-\gamma_{wf}\nabla D\right)\right]-\nabla\cdot\left(J^{\mathrm{Mol}}_{w,c,f}+J^{\mathrm{Disp}}_{w,c,f}\right)\\+\hat{q}_{T,c,f}\end{array}\right\},\quad\ldots\ldots(47a)$$

$$\hat{q}_{T,c,f}=x_c\xi_o\hat{q}_o+y_c\xi_g\hat{q}_g+w_c\xi_w\hat{q}_w,\quad\ldots\ldots(47b)$$

$$\tau_{T,c,f/m}=\left\{\begin{array}{l}x_c\xi_o\tau_o+y_c\xi_g\tau_g+w_c\xi_w\tau_w\\+\sigma\left[\left(\frac{S_g\phi_m}{\bar{\tau}}\right)\xi_{g,f/m}\right]D^{\mathrm{Mol}}_{o.c}\left(y_{c,f}-y^*_{c.m}\right)\end{array}\right\},\quad\ldots\ldots(48)$$

$$\tau_w=\sigma k_m\lambda_{wf/m}\left[\begin{array}{l}\left(p_{of}-p_{om}\right)\\+\frac{\sigma_z}{\sigma}\gamma_w\left(h_{wf}-h_{wm}\right)-\left(p_{cwof}-p_{cwom}\right)\end{array}\right],\quad\ldots\ldots(49)$$

$$\tau_g=\sigma k_m\lambda_{gf/m}\left[\begin{array}{l}\left(p_{of}-p_{om}\right)\\-\frac{\sigma_z}{\sigma}\gamma_g\left(h_{gf}-h_{gm}\right)+\left(p_{cgof}-p_{cgom}\right)\end{array}\right],\quad\ldots\ldots(50)$$

TABLE 1—MATRIX-BLOCK AND GRID DATA USED IN CASE 1	
Matrix-block dimensions (ft × ft × ft)	50 × 50 × 20
Porosity (fraction)	0.20
Matrix permeability (md)	3.20
Maximum capillary pressure (psi)	2.84
Oil viscosity (cp)	2.00
Water viscosity (cp)	1.00
Oil density (lbm/ft^3)	50.00
Water density (lbm/ft^3)	62.40
Number of grids for each direction	7 × 7 × 7
Matrix wettability	water-wet
S_{orw} (fraction)	0.20
S_{wi}/S_{wr} (fraction)	0.25

$$\tau_o = \sigma k_m \lambda_{of/m} \left\{ \begin{array}{l} (p_{of} - p_{om}) \\ +\frac{\sigma_z}{\sigma}\gamma_o\left[(h_{wf} - h_{wm}) - (h_{gf} - h_{gm})\right] \end{array} \right\}, \quad \ldots\ldots (51)$$

$$c_\phi = \frac{1}{\phi}\frac{\partial \phi}{\partial p}, \quad \ldots\ldots (52)$$

$$c_{vT} = -\frac{1}{v_T}\left(\frac{\partial v_T}{\partial p}\right)_{T,N}, \quad \ldots\ldots (53)$$

$$v_T = \frac{1}{\xi_o S_o + \xi_g S_g + \xi_w S_w}, \quad \ldots\ldots (54)$$

$$J^{\text{Mol}}_{o,c} = -\xi_o S_o \phi \sum_{n=1}^{N_c-1} \frac{D^{\text{Mol}}_{o,c,n}}{\tilde{\tau}} \nabla x_n, \quad \ldots\ldots (55)$$

$$J^{\text{Mol}}_{o,N_c} = -\sum_{k=1}^{N_c-1} J^{\text{Mol}}_{o,k}, \quad \ldots\ldots (56)$$

$$J^{\text{Mol}}_{g,c} = -\xi_g S_g \phi \sum_{k=1}^{N_c-1} \frac{D^{\text{Mol}}_{g,c,n}}{\tilde{\tau}} \nabla y_n, \quad \ldots\ldots (57)$$

$$J^{\text{Mol}}_{g,N_c} = -\sum_{k=1}^{N_c-1} J^{\text{Mol}}_{g,k}, \quad \ldots\ldots (58)$$

$$J^{\text{Mol}}_{w,c} = -\xi_w S_w \phi \frac{D^{\text{Mol}}_{w,c}}{\tilde{\tau}} \nabla w_c, \quad \ldots\ldots (59)$$

and

$$J^{\text{Disp}}_{o,c} = [J^{\text{Disp}}_{o,c}]_{i,j} = \left\{ \begin{array}{l} \left[\begin{array}{l} (\alpha_l - \alpha_t)_o |v_{o,i} v_{o,j}|/|\vec{v}_o| \\ +\alpha_{t,o}|\vec{v}_o| \end{array} \right] \\ +(\alpha_l - \alpha_t)_o |v_{o,i} v_{o,j}|/|\vec{v}_o| \end{array} \right\} \delta_{ij}, \quad \ldots\ldots (60)$$

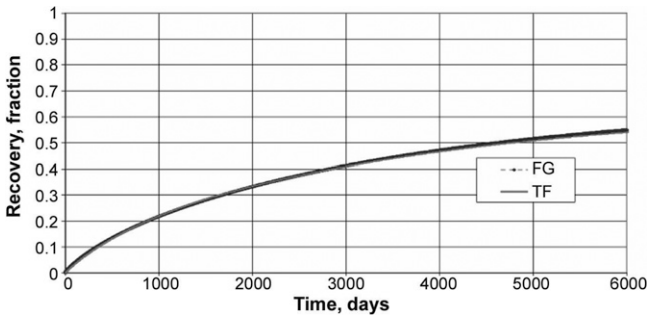

Fig. 5—Matrix oil recovery as a function of time for Case 1, after Balogun et al. (2007).

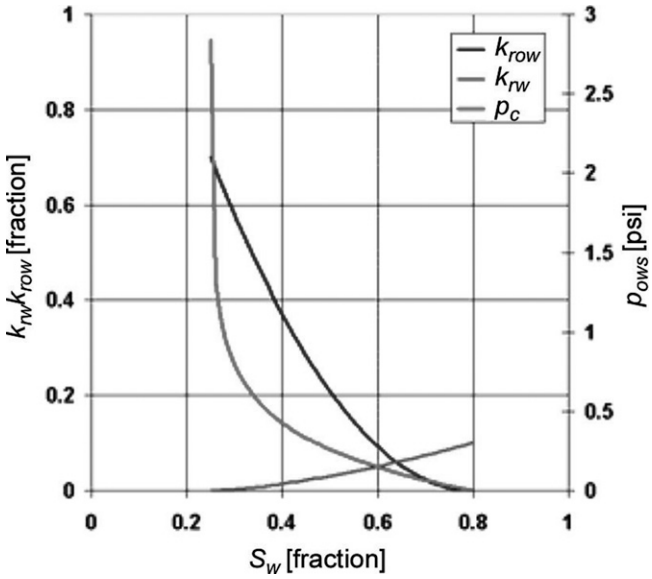

Fig. 4—Relative permeability and capillary pressure used in simulation, after Balogun et al. (2007).

where
$c = 1, 2 \ldots N_c$,
$i = 1, 2, 3 = x, y, z$,
$j = 1, 2, 3 = x, y, z$.

Analysis of Results

Water/Oil Simulation. Several water/oil-displacement numerical experiments were designed to calculate the oil drainage from the matrix using a fine-grid simulation and the single-cell transfer-function computation for the same matrix block. The numerical-model experiments covered a variety of situations by altering the matrix size, wettability, capillary pressure, and the boundary conditions. An extensive set of results were presented in an earlier paper (Balogun et al. 2007), but for this paper only one example (Case 1) is presented.

Table 1 shows the rock and fluid properties of the matrix block for Case 1. **Fig. 4** shows the relative permeability and capillary pressure curves used in the models. **Fig. 5** shows the oil recovery obtained from the transfer function and from the fine-grid model. It can be observed that there is close agreement between the two models.

Gas/Oil Simulation. The numerical model to study a gas-invoked oil drainage from a matrix block was constructed using a multicomponent-fluid system shown in **Tables 2 through 6.**

TABLE 2— INITIAL CONDITIONS AND ROCK/FLUID PROPERTIES	
ϕ_{fracture}	0.0056
ϕ_{matrix}	0.2000
Initial average pressure (psi)	3,897.3
Initial saturation pressure (psi)	2,492.0
Temperature (°F)	160.00
Initial oil saturation	0.8000
Initial water saturation	0.2000
Initial oil viscosity (cp)	0.2400
Initial gas viscosity (cp)	0.0238
Initial oil density (lbm/ft^3)	35.256
Initial gas density (lbm/ft^3)	11.5238

TABLE 3—COMPOSITIONAL DATA

	C_1	C_3	C_6	C_{10}	C_{15}	C_{20}
Initial overall composition	0.500	0.0300	0.0700	0.2000	0.1500	0.05
Gas-diffusion coefficient (ft^2/D)	0.100	0.0603	0.0431	0.0328	0.0279	0.00
Oil-diffusion coefficient (ft^2/D)	0.001	0.0006	0.0004	0.0003	0.0003	0.00
Molecular weight (lbm/lbm mol)	16.04	44.10	86.18	149.290	206.00	282.00

The matrix block has dimensions of 20×18×20 ft in the *x*-*y*-*z* coordinates, respectively, with a porosity of 0.20 and permeability of 100 md. A vertical *x*–*z* fracture was placed in the center of the matrix block, with a fracture permeability of 10,000 md and porosity of 0.0056. Gas was injected from the top of the fracture at a constant rate of 100 Mscf/D and was produced from the bottom of the fracture at a constant pressure. The grid dimension was 1 ft both in the vertical direction (*z*) and perpendicular to the fracture plane (*y*). The top and the bottom of the matrix, except for the fracture cross section, were sealed to gas flow. Thus, gas could enter the matrix only through the fracture face, and oil from the matrix could be produced through the fracture face.

Eclipse 300 (Schlumberger; Houston; 2005a) was used to generate oil drainage vs. time. The oil recovery from the matrix for four levels of gas/oil capillary holdup pressure (or the capillary threshold) is shown in **Fig. 6.** The gas-/oil-saturation distributions at the end of the experiments are shown in **Fig. 7.** These two figures clearly show the enormous sensitivity of oil drainage to the capillary holdup pressure.

To determine the effect of the molecular diffusion, both as a mixing mechanism and as a mass-transport vehicle, simulations were conducted and the results are shown in **Fig. 8.** It can be seen clearly that the molecular diffusion effect is rather small.

In fact, if one calculates the effective molecular diffusion from Eqs. 55 and 57 and compare it with the dispersion coefficient from Eq. 60, one sees that even for interstitial velocities as low as 1 ft/D, the molecular diffusion is insignificant.

Finally, we used the following gas/oil-transfer-function material-balance equation to calculate oil recovery from the matrix. The results are shown in **Fig. 9**, which compare extremely well with the simulation results shown earlier. Note that there is a difference in the ultimate recovery, which is caused by the fact that Eq. 61 does not include the compositional effects taken into account in the fine-grid simulation runs.

$$- \sigma k_m \frac{\lambda^n_{g,f/m}\lambda^n_{o,m/f}}{\lambda^n_T}\left[\begin{array}{l} -\left(p^n_{cgom}-p^n_{cgof}\right) \\ +\left(\frac{\sigma_z}{\sigma}\right)\left(\gamma^n_o-\gamma^n_g\right)\left(h^n_{gf}-h^n_{gm}\right)\end{array}\right] \simeq \phi_m \frac{S^{n+1}_o - S^n_o}{\Delta t}. \quad (61)$$

By comparing the transfer functions of this paper with the 1D gas/oil-gravity-drainage theory [Eq. 5 (Al-Kandari 2002)], and the numerical results of this work, we believe that when flow is dominated by gravity drainage, then σ should be set equal to σ_z; thus σ_z/σ becomes 1. In Part II of this paper (Al-Kobaisi et al. 2009), we expand Eq. 5 by finite differences to show why σ_z/σ, for gravity-drainage-dominated situations, becomes 1.

Conclusions

The objective of this paper is to provide a critical review and proper use of the matrix/fracture transfer functions by comparing their output to the output of the fine-grid matrix-block simulation. The following is a relevant summary:

- A set of transfer functions is provided for various applications to simulate and calculate oil recovery from a matrix block in dual-porosity models. The transfer-function approach is shown to be accurate and computationally more economical than fine gridding the matrix blocks.
- For immiscible flow, the transfer functions clearly show that oil drainage from a matrix block is overwhelmingly controlled by capillary and gravity forces. Viscous displacement is not typically accounted for in many dual-porosity simulators and, in general, is negligible. Oil production by fluid expansion can also be accounted for by means of a transfer-function approach.

TABLE 4—GAS-SATURATION FUNCTIONS

S_g	k_{rg}	p_{cog} (psi)
0.000	0.000	2.000
0.050	0.000	2.160
0.089	0.001	2.292
0.178	0.010	2.623
0.267	0.030	3.006
0.356	0.050	3.458
0.444	0.100	4.011
0.533	0.200	4.724
0.622	0.350	5.730
0.650	0.390	6.151
0.711	0.560	7.449
0.800	1.000	29.99

TABLE 5—OIL RELATIVE PERMEABILITIES

S_o	k_{row}	k_{rog}
0.000	0.000	0.000
0.089	0.000	0.000
0.150	0.000	0.000
0.178	0.000	0.011
0.267	0.000	0.037
0.300	0.000	0.056
0.356	0.012	0.088
0.444	0.084	0.172
0.533	0.218	0.296
0.622	0.415	0.471
0.711	0.677	0.702
0.800	1.000	1.000

TABLE 6—WATER-SATURATION FUNCTIONS		
S_w	k_{rw}	p_{cwo} (psi)
0.200	0.000	45.00
0.290	0.002	19.03
0.378	0.018	10.07
0.467	0.061	4.900
0.556	0.144	1.800
0.644	0.281	0.500
0.700	0.409	0.050
0.733	0.486	0.010
0.822	0.771	0.000
0.911	1.000	0.000
1.000	1.000	0.000

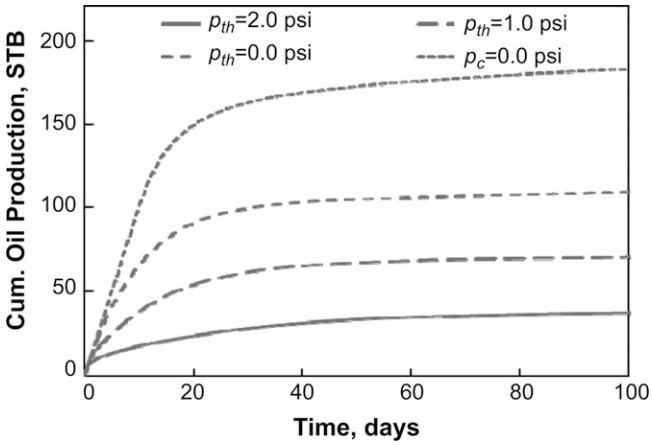

Fig. 6—Oil recovery as a function of capillary holdup pressure.

- For typical production times, molecular diffusion has a very minor effect on oil recovery from matrix blocks. Molecular diffusion, however, has significant long-term effects on component redistribution or gas production from nanodarcy rocks.
- For miscible flow, the fracture/matrix mass transfer is less complicated because there is no capillary force, say, between the solvent (gas) and oil; nevertheless, gravity contrast between solvent flowing in the fracture and oil residing in the matrix creates convective mass transfer between fracture and matrix by gravity. For the immiscible case, the gas enters the matrix from the highest fracture contact point, while in the miscible case the solvent (gas) could enter at any point, but upon entry it will try to rise to the top of the matrix. In this journey, the solvent mixes with the oil and oil composition changes rapidly.

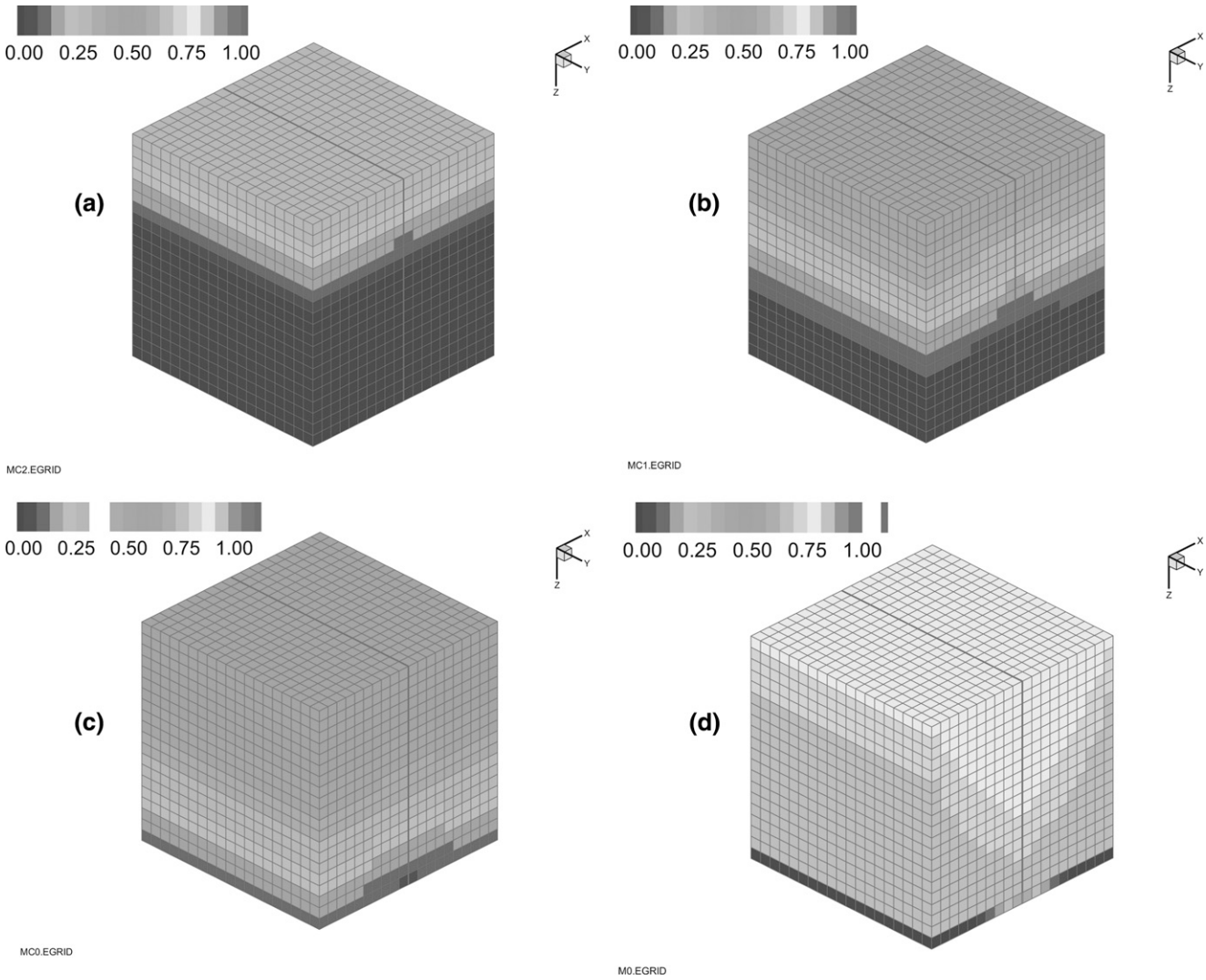

Fig. 7—Gas-saturation profile for p_{th} = 2.0 (a); p_{th} = 1.0 (b); p_{th} = 0.0 (c); and p_c = 0.0 (d).

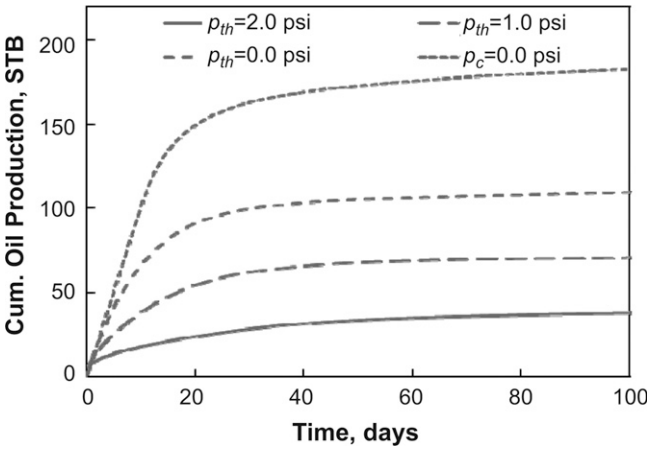

Fig. 8—Oil recovery as a function of capillary holdup and molecular diffusion (compare to Fig. 6).

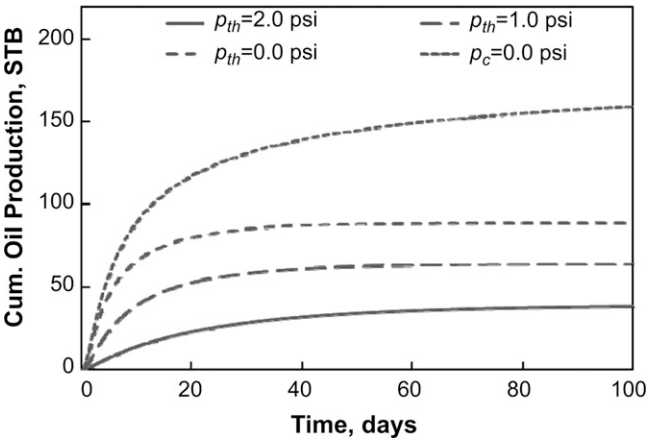

Fig. 9—Transfer-function oil recoveries.

Nomenclature

A = area of an open surface of a matrix block or cross sectional area normal to flow, ft^2
c = compressibility, psi^{-1}
d = distance from the center of a matrix block to an open bounding surface, ft
D = depth, ft
D_m = molecular diffusion, ft^2/D
$\hat{D}_{pc}$ = capillary dispersion coefficient for gas-oil flow, ft^2/D
f = fractional flow, fraction
$\hat{f}$ = fractional flow for gas/oil gravity drainage, fraction
h = gravity head, ft
J = molecular diffusion and/or hydrodynamic dispersion mass vector, lbm mol/D
k = 0.006328 × absolute permeability, md
k_f = 0.006328 × absolute fracture permeability, md
k_r = relative permeability
k_r^* = relative permeability endpoint
k_{ro}^* = maximum relative permeability to oil
k_{rw}^* = maximum relative permeability to water
l = characteristic length of a matrix block, ft
L = matrix-block dimension, ft
n = number of fracture sets
n_o = oil exponent
n_w = water exponent
N_c = total number of components
p = phase pressure, psi
q = reservoir-flow rate, ft^3/D
$\hat{q}$ = reservoir flow rate per rock volume, day^{-1} or lbm mol/ft^3·day
RF = recovery factor, fraction
S = saturation, fraction
S_{gD} = dimensionless gas saturation, fraction
S_{oD} = dimensionless oil saturation, fraction
S_{orw} = residual-oil saturation to water, fraction
S_{wD} = dimensionless water saturation, fraction
S_{wr} = irreducible water saturation, fraction
t = time, days
$\hat{u}$ = interstitial free fall velocity for the oil phase, ft/D
$\vec{u}$ = interstitial velocity vector, ft/D
v = darcy velocity, ft/D
$\vec{v}$ = darcy velocity vector, ft/D
v_T = specific total volume, ft^3/lbm mol
$\bar{v}_{T,c}$ = partial total molar volume for comp c, ft^3/lbm mol
V = volume of a matrix block, ft^3
VR = volume of a gridblock, ft^3
w_c = mole fraction of water component c, fraction
x_c = mole fraction of oil component c, fraction
y_c = mole fraction of gas component c, fraction
y_c^* = mole fraction of gas component c for saturated-oil phase at pressure p, fraction
z_c = total mole fraction of component c, fraction
α_l = longitudinal dispersion coefficient, ft
α_t = tranversal dispersion coefficient, ft
γ = fluid gravity gradient, psi/ft
Δt = time step, days
Δx = x-direction grid dimension, ft
Δy = y-direction grid dimension, ft
Δz = z-direction grid dimension, ft
λ = mobility coefficient, cp^{-1}
μ = viscosity, cp
ξ = molar density, lbm/lbm mol
ρ = density, lbm/ft^3
σ = matrix block shape facture, 1/ft^2
τ = matrix/fracture transfer function, day^{-1}
$\tilde{\tau}$ = tortuosity, dimensionless
ϕ = porosity, fraction

Subscripts

c = component
f = fracture
g = gas
m = matrix
o = oil
pc = capillary
w = water
T = total
x = x-direction index
y = y-direction index
z = z-direction index
ϕ = pore

Acknowledgments

This research was conducted at the Marathon Center of Excellence for Reservoir Studies (MCERS) at Colorado School of Mines. We acknowledge the funding by Marathon Oil Corporation, Saudi Aramco, PEMEX, ADNOC, and Repsol-YPF. We also acknowledge the computing resources provided by Marathon Oil Corporation to conduct the simulation studies.

References

Acs, G., Doleschall, S., and Farkas, E. 1985. General Purpose Compositional Model. *SPE J.* **25** (4) 543–553. SPE-10515-PA. DOI: 10.2118/10515-PA.

Al-Kandari, H.A. 2002. Numerical simulation of gas-oil gravity drainage for centrifuge experiments and scaled reservoir matrix blocks. PhD dissertation, Colorado School of Mines, Golden, Colorado.

Al-Kandari, H.A., Kazemi, H., and Van Kirk, C.W. 2002. Gas Injection Enhanced Oil Recovery in High Relief Naturally Fractured Reservoirs. Presented at the Kuwait International Petroleum Conference and Exhibition, Kuwait City, State of Kuwait, 14–16 December.

Al-Kobaisi, M., Kazemi, H., Ramirez, B., Ozkan, E., and Atan, S. 2009. A Critical Review for Proper Use of Water/Oil/Gas Transfer Functions in Dual-Porosity Naturally Fractured Reservoirs: Part II. *SPE Res Eval & Eng* **12** (2): 211–217. SPE-11778-PA. DOI: 10.2523/11778-PA.

Balogun, A., Kazemi, H., Ozkan, E., Al-Kobaisi, A., and Ramirez, B. 2007. Verification and Proper Use of Water/Oil Transfer Function for Dual-Porosity and Dual-Permeability Reservoirs. Paper SPE 104580 presented at the SPE Middle East Oil and Gas Show and Conference, Kingdom of Bahrain, 11–14 March. DOI: 10.2118/104580-MS.

Barenblatt, G.I., Zheltov, I.P., and Kochina, I.N. 1960. Basic concepts in the theory of seepage of homogeneous liquids in fissured rocks. *J. of Applied Mathematics and Mechanics* **24** (5): 1286–1303. DOI:10.1016/0021-8928(60)90107-6.

Beliveau, D. 1989. Pressure Transients Characterize Fractured Midale Unit. *J. Pet Tech* **41** (12): 1354–1362; *Trans.,* AIME, **287.** SPE-15635-PA. DOI: 10.2118/15635-PA.

Blair, P.M. 1964. Calculation of Oil Displacement by Countercurrent Water Imbibition. *SPE J.* **4** (3): 195–202; *Trans.,* AIME, **231.** SPE-873-PA. DOI: 10.2118/873-PA.

Chang, M.-M. 1993. NIPER-696: Deriving the shape factor of a fractured rock matrix. Technical report, Contract No. DE93000170, US DOE, Washington, DC (September 1993). DOI: 10.2172/10192737.

Civan, F. and Rasmussen, M.L. 2002. Analytical Hindered-Matrix-Fracture Transfer Models for Naturally Fractured Petroleum Reservoirs. Paper SPE 74364 presented at the SPE International Petroleum Conference and Exhibition in Mexico, Villahermosa, Mexico, 10–12 February. DOI: 10.2118/74364-MS.

Fung, L.S.K. 1991. Simulation of Block-to-Block Processes in Naturally Fractured Reservoirs. *SPE Res Eng* **6** (4): 477–484. SPE-20019-PA. DOI: 10.2118/20019-PA.

Gilman, J.R. 1986. An Efficient Finite-Difference Method for Simulating Phase Segregation in the Matrix Blocks in Double-Porosity Reservoirs. *SPE Res Eng* **1** (4): 403–413; *Trans.,* AIME, **281.** SPE-12271-PA. DOI: 10.2118/12271-PA.

Gilman, J.R. 2003. Practical aspects of simulation of fractured reservoirs. Presented at the International Forum on Reservoir Simulation, Buhl, Baden-Baden, Germany, 23–27 June.

Gilman, J.R. and Kazemi, H. 1988. Improved Calculations for Viscous and Gravity Displacement in Matrix Blocks in Dual-Porosity Simulators. *J. Pet Tech* **40** (1): 60–70; *Trans.,* AIME, **285.** SPE-16010-PA. DOI: 10.2118/16010-PA.

Hagoort, J. 1980. Oil Recovery by Gravity Drainage. *SPE J.* **20** (3): 139–150. SPE-7424-PA. DOI: 10.2118/7424-PA.

Heinemann, Z.E. and Mittermeir, M.G. 2006. Rigorous derivation of the Kazemi-Gilman-Elsharkawy generalized dual-porosity shape factor. Paper B044 presented at the European Conference on the Mathematics of Oil Recovery, Amsterdam, 4–7 September.

Horie, T., Firoozabadi, A., and Ishimoto, K. 1990. Laboratory Studies of Capillary Interaction in Fracture/Matrix Systems. *SPE Res Eng* **5** (3): 353–360. SPE-18282-PA. DOI: 10.2118/18282-PA.

Hoteit, H. and Firoozabadi, A. 2006. Numerical Modeling of Diffusion in Fractured Media for Gas Injection and Recycling Schemes. Paper SPE 103292 presented at the SPE Annual Technical Conference and Exhibition, San Antonio, Texas, USA, 24–27 September. DOI: 10.2118/103292-MS.

Iffly, R., Rousselet, D.C., and Vermeulen, J. L. 1972. Fundamental Study of Imbibition in Fissured Oil Fields. Paper SPE 4102 presented at the SPE Annual Meeting, San Antonio, Texas, USA, 8–11 October. DOI: 10.2118/4102-MS.

Kazemi, H. and Gilman, J.R. 1993. Multiphase flow in fractured petroleum reservoirs. In *Flow and Contaminant Transport in Fractured Rock*, ed. J. Bear, C.-F. Tsang, G. de Marsily, 267–323. San Diego, California: Academic Press.

Kazemi, H., Merrill, J.R., Porterfield, K.L., and Zeman, P.R. 1976. Numerical Simulation of Water-Oil Flow in Naturally Fractured Reservoirs. *SPE J.* **16** (6): 317–326; *Trans.,* AIME, **261.** SPE-5719-PA. DOI: 10.2118/5719-PA.

Kleppe, J. and Morse, R.A. 1974. Oil Production From Fractured Reservoirs by Water Displacement. Paper SPE 5084 presented at the SPE Meeting, Houston, 6–9 October. DOI: 10.2118/5084-MS.

Kyte, J.R. 1970. A Centrifuge Method To Predict Matrix-Block Recovery in Fractured Reservoirs. *SPE J.* **10** (2): 161–170; *Trans.,* AIME, **249.** SPE-2729-PA. DOI: 10.2118/2729-PA.

Lim, K.T. and Aziz, K. 1995. Matrix-fracture transfer functions for dual porosity simulators. *J. Pet. Sci. Eng.* **13** (3–4): 169–178. DOI: 10.1016/0920-4105(95)00010-F.

Litvak, B.L. 1985. Simulation and characterization of naturally fractured reservoirs. *Proc.,* Reservoir Characterization Technical Conference, Dallas, 561–583.

Lu, H., Di Donato, G., and Blunt, M.J. 2006. General Transfer Functions for Multi-Phase Flow. Paper SPE 102542 presented at the SPE Annual Technical Conference and Exhibition, San Antonio, Texas, USA, 24–27 September. DOI: 10.2118/102542-MS.

Mattax, C.C. and Kyte, J.R. 1962. Imbibition Oil Recovery From Fractured, Water-Drive Reservoir. *SPE J.* **2** (2): 177–184; *Trans.,* AIME, **225.** SPE-187-PA. DOI: 10.2118/187-PA.

Rangel-German, E.R. and Kovscek, A.R. 2003. Time-Dependent Matrix-Fracture Shape Factors for Partially and Completely Immersed Fractures. Paper SPE 84411 presented at the SPE Annual Technical Conference and Exhibition, Denver, 5–8 October. DOI: 10.2118/84411-MS.

Saidi, A.M. 1983. Simulation of Naturally Fractured Reservoirs. Paper SPE 12270 presented at the SPE Reservoir Simulation Symposium, San Francisco, 15–18 November. DOI: 10.2118/12270-MS.

Sonier, F., Souillard, P., and Blaskovich, F.T. 1988. Numerical Simulation of Naturally Fractured Reservoirs. *SPE Res Eng* **3** (4): 1114–1122; *Trans.,* AIME, **285.** SPE-15627-PA. DOI: 10.2118/15627-PA.

Uleberg, K. and Kleppe, J. 1996. Dual porosity, dual permeability formulation for fractured reservoir simulation. Presented at the Norwegian University of Science and Technology, Trondheim RUTH Seminar, Stavanger.

Warren, J.E. and Root, P.J. 1963. The Behavior of Naturally Fractured Reservoirs. *SPE J.* **3** (3): 245–255; *Trans.,* AIME, **228.** SPE-426-PA. DOI: 10.2118/426-PA.

Watts, J.W. 1986. A Compositional Formulation of the Pressure and Saturation Equations. *SPE Res Eng* **1** (3): 243–252; *Trans.,* AIME, **281.** SPE-12244-PA. DOI: 10.2118/12244-PA.

Wong, T.W., Firoozabadi, A., and Aziz, K. 1990. Relationship of the Volume-Balance Method of Compositional Simulation to the Newton-Raphson Method. Paper SPE 21462 (supplement to paper SPE 18424) available from SPE, Richardson, Texas, USA.

Yamamoto, R.H., Padgett, J.B., Ford, W.T., and Boubeguira, A. 1971. Compositional Reservoir Simulation for Fissured Systems—The Single-Block Model. *SPE J.* **11** (2): 113–128. SPE-2666-PA. DOI: 10.2118/2666-PA.

Zhang, X., Morrow, N.R., and Ma, S. 1996. Experimental Verification of a Modified Scaling Group for Spontaneous Imbibition. *SPE Res Eng* **11** (4): 280–285. SPE-30762-PA. DOI: 10.2118/30762-PA.

SI Metric Conversion Factors

cp	× 1.0*	E – 03 = Pa·s
ft	× 3.048*	E – 01 = m
ft^2	× 9.290 304*	E – 02 = m^2
ft^3	× 2.831 685	E – 02 = m^3
°F	(°F – 32)/1.8	= °C
lbm	× 4.535 924	E – 01 = kg
psi	× 6.894 757	E + 00 = kPa

*Conversion factor is exact.

Benjamin Ramirez is a reservoir engineer with Marathon Oil Corporation. He holds a BS in mechanical engineering from U. de los Andes and an MS in petroleum engineering from the Colorado School of Mines. **Hossein Kazemi** is the Chesebro' Distinguished Professor of Petroleum Engineering at Colorado School of Mines and Codirector of MCERS. He holds BS and PhD degrees in petroleum engineering from the U. of Texas at Austin in (1961 and 1963, respectively). Kazemi is a member of the National Academy of Engineering, a distinguished and an honorary member of SPE. He has published numerous technical papers and has served as a distinguished author and speaker for SPE. Kazemi retired from Marathon Oil Corporation in 2001 after serving as research scientist, senior technical consultant, director of production research, manager of reservoir technology, and executive technical fellow at Marathon Petroleum Technology Center in Littleton, Colorado. At Colorado School of Mines, he has taught graduate courses in petroleum engineering and supervised graduate research in reservoir modeling, well testing, and improved oil and gas recovery. **Mohammed Al-Kobaisi** is a reservoir engineer with Abu Dhabi National Oil Company. He holds BS and MS degrees in petroleum engineering from Colorado School of Mines, where he is currently a PhD candidate. **Erdal Ozkan** is a professor of petroleum engineering and codirector of MCERS at Colorado School of Mines. He holds BS and MS degrees from Istanbul Technical U. and a PhD degree from the U. of Tulsa, all in petroleum engineering. Since 1989, Ozkan has taught at Istanbul Technical U. and Colorado School of Mines. His main research interests are pressure-transient analysis, modeling fluid flow in porous media, horizontal and multilateral well technology, and unconventional reservoirs. Ozkan served as the Executive Editor of *SPE Res Eval & Eng* and as the Editor in Chief of Elsevier B.V. *J. of Petroleum Science and Engineering*. He is the recipient of the 2007 SPE Formation Evaluation Award. **Safian Atan** is a reservoir engineer with Marathon Oil Corporation. He holds BS, ME, and PhD degrees in petroleum engineering from Colorado School of Mines.